Disasters due to Unplanned Urbanisation

T. V. Ramachandra

Introduction

Urbanisation is a form of metropolitan growth that is a response to often bewildering sets of economic, social, and political forces and to the physical geography of an area. It is the increase in the population of cities in proportion to the region's rural population. The 20th century is witnessing "the rapid urbanisation of the world's population", as the global proportion of urban population rose dramatically from 13% (220 million) in 1900, to 29% (732 million) in 1950, to 49% (3.2 billion) in 2005 and is projected to rise to 60% (4.9 billion) by 2030 (World Urbanization Prospects, 2005). Urban ecosystems are the consequence of the intrinsic nature of humans as social beings to live together (Sudhira *et al*., 2003; Ramachandra and Uttam Kumar, 2008). The process of urbanisation contributed by infrastructure initiatives, consequent population growth and migration results in the growth of villages into towns, towns into cities and cities into metros. Urbanisation and urban sprawl have posed serious challenges to the decision makers in the city planning and management process involving plethora of issues like infrastructure development, traffic congestion, and basic amenities (electricity, water, and sanitation), etc. (Kulkarni and Ramachandra, 2006). Apart from this, major implications of urbanisation are:

- **Loss of wetlands:** Urbanisation has telling influences on the natural resources such as decline in number of wetlands and / or depleting groundwater table.
- **Floods:** Common consequences of urban development are increased peak discharge and frequency of floods as land is converted from fields or woodlands to roads and parking lots, it loses its ability to absorb rainfall. Conversion of water bodies to residential layouts has compounded the problem by removing the interconnectivities in an undulating terrain. Encroachment of natural drains, alteration of topography involving

Energy & Wetlands Research Group, Centre for Ecological Sciences, & Centre for Sustainable Technologies,
Centre for infrastructure, Sustainable Transportation and Urban Planning (CiSTUP) Indian Institute of Science Bangalore

E-mail: cestvr@ces.iisc.ernet.in, energy@ces.iisc.ernet.in, http://ces.iisc.ernet.in/energy

the construction of high rise buildings, removal of vegetative cover, reclamation of wetlands are the prime reasons for frequent flooding even during normal rainfall post 2000.

- **Decline in groundwater table:** Studies reveal the removal of waterbodies has led to the decline in water table. Water table has declined to 300 m from 28 m over a period of 20 years after the reclamation of lake with its catchment for commercial activities. Also, groundwater table in intensely urbanized area such as whitefield, etc. has now dropped to 400 to 500m.
- **Loss of tree cover**: Drastic reduction in cover is observed due to the removal of lane tress and conversion of plantations to layouts, etc.
- **Heat island:** Surface and atmospheric temperatures are increased by anthropogenic heat discharge due to energy consumption, increased land surface coverage by artificial materials having high heat capacities and conductivities, and the associated decreases in vegetation and water pervious surfaces, which reduce surface temperature through evapotranspiration.
- **Increased carbon footprint**: Due to the adoption of inappropriate building architecture, the consumption of electricity has increased in certain corporation wards drastically. The building design conducive to tropical climate would have reduced the dependence on electricity. Higher energy consumption, enhanced pollution levels due to the increase of private vehicles, traffic bottlenecks have contributed to carbon emissions significantly. Apart from these, mismanagement of solid and liquid wastes has aggravated the situation.

Unplanned urbanisation has drastically altered the drainage characteristics of natural catchments, or drainage areas, by increasing the volume and rate of surface runoff. Drainage systems are unable to cope with the increased volume of water and are often encountered with the blockage due to indiscriminate disposal of solid wastes. Encroachment of wetlands, floodplains, etc. obstructs floodways causing loss of natural flood storage. Damages from urban flooding could be categorized as: direct damage – typically material damage caused by water or flowing water, and indirect damage – e.g. traffic disruptions, administrative and labour costs, production losses, spreading of diseases, etc.

Studies on the phenomenon of Urban Heat Island (UHI) using satellite derived land surface temperature (LST) measurements have been conducted using various satellite data products acquired in thermal region of the electromagnetic spectrum. Currently available satellite thermal infrared sensors provide different spatial resolution and temporal coverage data that can be used to estimate LST. The Geostationary Operational Environmental Satellite (GOES) has a 4-km resolution in the thermal infrared, while the NOAA-Advanced Very High Resolution Radiometer (AVHRR) and the Terra and Aqua-MODIS have 1-km spatial

resolutions. Significantly high resolution data come from the Terra-Advanced Spaceborne Thermal Emission and Reflection Radiometer (ASTER) which has a 90-m pixel resolution, the Landsat-5 Thematic Mapper (TM) which has a 120-m resolution, and Landsat-7 Enhanced Thematic Mapper (ETM) which has a 60-m resolution. However, these instruments have a repeat cycle of 16 days (Li *et. al.,* 2004; Ramachandra and Uttam Kumar, 2009). Weng (2001, 2003) examined LST pattern and its relationship with land cover (LC) in Guangzhou and in the urban clusters in the Zhujiang Delta, China. Nikolakopopulos *et al*., (2003) have used Landsat-5 TM and Landsat-7 ETM+ data for creating the temperature profile of Alfios River Basin. Stathopoulou and Cartalis (2007) have used Landsat ETM+ data to identify daytime urban heat island using Corine LC data for major cities in Greece. Using a Landsat ETM+ imagery of City of Indianapolis, IN, USA, Weng *et al.,* (2004) examined the surface temperature UHI in the city. They derived LST and analysed their spatial variations using Landsat ETM+ thermal measurements with the urban vegetation abundance and investigated their relationship. UHI studies have traditionally been conducted for isolated locations and with in situ measurements of air temperatures. The advent of satellite remote sensing technology has made it possible to study UHI both remotely and on continental or global scales (Streutker, 2002). In this work, Landsat data of 1973 (of 79 m spatial resolution), 1992 and 2000 (30 m), IRS LISS-III data of 1999 and 2006 (23.5 m) and MODIS data of 2002 and 2007 (with 250 m to 500 m spatial resolution) are used with supervised pattern classifiers based on maximum likelihood (ML) estimation. Also, an attempt is made to map land surface temperatures across various LC types to understand heat island effect.

Study Area

Greater Bangalore (77°37'19.54" E and 12°59'09.76" N) is the principal administrative, cultural, commercial, industrial, and knowledge capital of the state of Karnataka with an area of 741 sq. km. Bangalore city administrative jurisdiction was widened in 2006 by merging the existing area of Bangalore city spatial limits with 8 neighbouring Urban Local Bodies (ULBs) and 111 Villages of Bangalore Urban District (Ramachandra and Uttam Kumar, 2008; Sudhira *et al.*, 2007). Thus, Bangalore has grown spatially more than ten times since 1949 (69 square kilometers) and is a part of both the Bangalore urban and rural districts (figure 1). Now, Bangalore is the fifth largest metropolis in India currently with a population of about 7 million (figure 2). The mean annual total rainfall is about 880 mm with about 60 rainy days a year over the last ten years. The summer temperature ranges from 18° C – 38° C, while the winter temperature ranges from 12° C – 25° C. Thus, Bangalore enjoys a salubrious climate all round the year. Bangalore is located at an altitude of 920 meters above mean sea level, delineating four watersheds, viz. Hebbal, Koramangala, Challaghatta and Vrishabhavathi watersheds. The

undulating terrain in the region has facilitated creation of a large number of tanks providing for the traditional uses of irrigation, drinking, fishing and washing. This led to Bangalore having hundreds of such water bodies through the centuries. Even in early second half of 20th century, in 1961, the number of lakes and tanks in the city stood at 262 (and spatial extent of Bangalore was 112 sq km). However, number of lakes and tanks in 1985 was 81 (and spatial extent of Bangalore was 161 sq km).

Figure 1: Study area – Greater Bangalore.

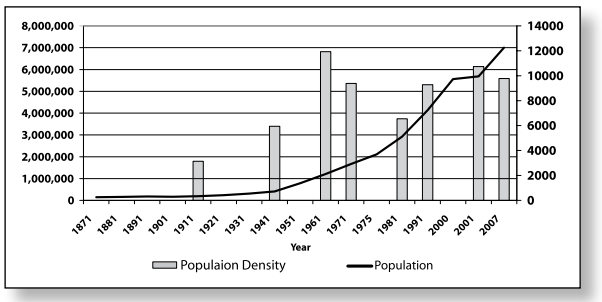

Figure 2: Population growth and population density.

Materials and Methods

Survey of India (SOI) toposheets of 1:50000 and 1:250000 scales were used to generate base layers. Field data were collected with a handheld GPS. Remote sensing data used for the study are: Landsat MSS (1973), Landsat TM (1992), Landsat ETM+ (2000 and 2009) [Land-

sat data downloaded from http://glcf.umiacs.umd.edu/data/], IRS (Indian Remote Sensing) LISS (Linear Imaging Self Scanner)-III of (1999 and 2006), MODIS (Moderate Resolution Imaging Spectroradiometer) Surface Reflectance 7 bands product [downloaded from http://edcdaac.usgs.gov/main.asp] of 2002, MODIS Land Surface Temperature/Emissivity 8-Day L3 Global and Daily L3 Global (V004 product) [http://lpdaac.usgs.gov/modis/dataproducts.asp#mod11]. Google Earth data (http://earth.google.com) served in pre and post classification process and validation of the results. The methods adopted in the analysis involved:

- Georeferencing of acquired remote sensing data to latitude-longitude coordinate system with Evrst 56 datum: Landsat bands, IRS LISS-III MSS bands, MODIS bands 1 and 2 (spatial resolution 250 m) and bands 3 to 7 (spatial resolution 500 m) were geo-corrected with the known ground control points (GCP's) and projected to Polyconic with Evrst 1956 as the datum, followed by masking and cropping of the study area.
  - Band 1, 2, 3 and 4 of Landsat 1973 data to 79 m.
  - Band 1, 2, 3 and 4 of Landsat TM of 1992 to 30 m.
  - Band 1, 2, 3, 4, 5 and 7 of Lansat ETM+ to 30 m.
  - MODIS bands 1 to 7 to 250 m.
  - IRS LISS-III band 1, 2 and 3 to 23.5 m.
  - Thermal band of TM (resampled to 120m), ETM+ (to 60m) and MODIS (to 1 km) and Panchromatic bands of ETM+ (resampled to 15 m).
- Supervised Classification using Bayesian Classifier: In supervised classification, the pixel categorisation process is done by specifying the numerical descriptors of the various LC types present in a scene. It involves (i) training, (ii) classification and (iii) output.
- Accuracy assessment: Accuracy assessments were done with field knowledge, visual interpretation and also referring Google Earth (http://earth.google.com).
- Computation of Normalised Difference Vegetation Index (NDVI): It separates green vegetation from its background soil brightness and retains the ability to minimize topographic effects while producing a measurement scale ranging from –1 to +1 with NDVI-values < 0 representing no vegetation.

Derivation of Land Surface Temperature (LST)

LST from Landsat TM: The TIR band 6 of Landsat-5 TM was used to calculate the surface temperature of the area. The digital number (DN) was first converted into radiance L_{TM} using

$$L_{TM} = 0.124 + 0.00563 * DN \quad \text{(Equation 1)}$$

The radiance was converted to equivalent blackbody temperature $T_{TMSurface}$ at the satellite using

$$T_{TMSurface} = K_2/(K_1 - \ln L_{TM}) - 273 \quad \text{(Equation 2)}$$

The coefficients K_1 and K_2 depend on the range of blackbody temperatures. In the blackbody temperature range 260-300K the default values (Singh, S. M., 1988) for Landsat TM are K_1 = 4.127 and K_2 = 1274.7. Brightness temperature is the temperature that a blackbody would obtain in order to produce the same radiance at the same wavelength (λ = 11.5 μm). Therefore, additional correction for spectral emissivity (ε) is required to account for the non-uniform emissivity of the land surface. Spectral emissivity for all objects are very close to 1, yet for more accurate temperature derivation emissivity of each LC class is considered separately. Emissivity correction is carried out using surface emissivities for the specified LC (table 1) derived from the methodology described in Snyder *et al*., (1998) and Stathopoulou *et al*. (2006).

Table 1*: Surface emissivity values by LC type*

LC type	Emissivity
Densely urban	0.946
Mixed urban (Medium Built)	0.964
Vegetation	0.985
Water body	0.990
Others	0.950

The procedure involves combining surface emissivity maps obtained from the Normalized Difference Vegetation Index Thresholds Method ($NDVI^{THM}$) (Sobrino and Raissouni, 2000) with LC information. The emmissivity corrected land surface temperature (Ts) were finally computed as follows (Artis and Carnhan, 1982)

$$T_s = \frac{T_B}{1 + (\lambda \times T_B / \rho) \ln \varepsilon} \quad \text{(Equation 3)}$$

where, λ is the wavelength of emitted radiance for which the peak response and the average of the limiting wavelengths (λ = 11.5 μm) were used, $\rho = h \times c/\sigma$ (1.438×10^{-2} mK), σ = Stefan Bolzmann's constant (5.67×10^{-8} $Wm^{-2}K^{-4}$ = 1.38×10^{-23} J/K), h = Planck's constant (6.626×10^{-34} Jsec), c = velocity of light (2.998×10^{8} m/sec), and ε is spectral emissivity.

LST from Landsat ETM+: The TIR image (band 6) was converted to a surface temperature map according to the following procedure (Weng *et al*., 2004). The DN of Landsat ETM+

was first converted into spectral radiance L_{ETM} using equation 4, and then converted to at-satellite brightness temperature (i.e., black body temperature, $T_{ETMSurface}$), under the assumption of uniform emissivity ($\varepsilon \approx 1$) using equation 5 (Landsat Project Science Office, 2002):

$$L_{ETM} = 0.0370588 \times DN + 3.2 \quad \text{(Equation 4)}$$

$$T_{ETMSurface} = K2/\ln (K_1/ L_{ETM} + 1) \quad \text{(Equation 5)}$$

where, $T_{ETMSurface}$ is the effective at-satellite temperature in Kelvin, L_{ETM} is spectral radiance in watts/(meters squared x ster x μm); and K_2 and K_2 are pre-launch calibration constants. For Landsat-7 ETM+, $K_2 = 1282.71$ K and $K_1 = 666.09$ $mWcm^{-2}sr\text{-}1\mu m^{-1}$ were used (http://ltpwww.gsfc.nasa.gov/IAS/handbook/handbook_htmls/chapter11/chapter11.html). The emissivity corrected land surface temperatures Ts were finally computed by equation 3.

Results and Discussion

The supervised classified images of 1973, 1992, 1999, 2000, 2002, 2006 and 2009 with an overall accuracy of 72%, 75%, 71%, 77%, 60%, 73% and 86% were obtained using the open source programs (i.gensig, i.class and i.maxlik) of Geographic Resources Analysis Support System (http://wgbis.ces.iisc.ernet.in/ grass) as displayed in figure 3. The class statistics is given in table 2. The implementation of the classifier on Landsat, IRS and MODIS image helped in the digital data exploratory analysis as were also verified from field visits in July, 2007 and Google Earth image. From the classified raster maps, urban class was extracted and converted to vector representation for computation of precise area in hectares. There has been a 632% increase in built up area from 1973 to 2009 leading to a sharp decline of 79% area in water bodies in Greater Bangalore mostly attributing to intense urbanisation process. Figure 4 shows Greater Bangalore with 265 water bodies (in 1972). The rapid development of urban sprawl has many potentially detrimental effects including the loss of valuable agricultural and eco-sensitive (e.g. wetlands, forests) lands, enhanced energy consumption and greenhouse gas emissions from increasing private vehicle use (Ramachandra and Shwetmala, 2009). Vegetation has decreased by 32% from 1973 to 1992, by 38% from 1992 to 2002 and by 63% from 2002 to 2009. Disappearance of water bodies or sharp decline in the number of waterbodies in Bangalore is mainly due to intense urbanisation and urban sprawl. Many lakes (54%) were unauthorised encroached for illegal buildings. Field survey (during July-August 2007) shows that nearly 66% of lakes are sewage fed, 14% surrounded by slums and 72% showed loss of catchment area. Also, lake catchments were used as dumping yards for either municipal solid waste or building debris. The surrounding of these lakes have illegal

constructions of buildings and most of the times, slum dwellers occupy the adjoining areas. At many sites, water is used for washing and household activities and even fishing was observed at one of these sites. Multi-storied buildings have come up on some lake beds that have totally intervene the natural catchment flow leading to sharp decline and deteriorating quality of waterbodies. This is correlated with the increase in built up area from the concentrated growth model focusing on Bangalore, adopted by the state machinery, affecting severely open spaces and in particular waterbodies. Some of the lakes have been restored by the city corporation and the concerned authorities in recent times.

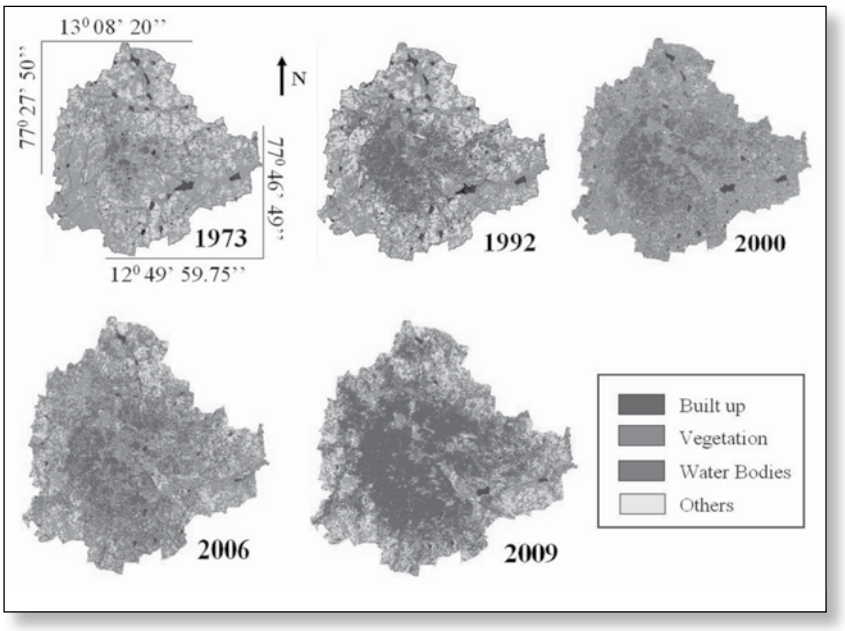

Figure 3: Greater Bangalore in 1973, 1992, 1999, 2000 and 2009.

***Table 2**: Greater Bangalore LC statistics*

Class / Year		Built up	Vegetation	Water Bodies	Others
1973	Ha	5448	46639	2324	13903
	%	7.97	68.27	3.40	20.35
1992	Ha	18650	31579	1790	16303
	%	27.30	46.22	2.60	23.86

Class / Year		Built up	Vegetation	Water Bodies	Others
1999	Ha	23532	31421	1574	11794
	%	34.44	45.99	2.30	17.26
2000	Ha	24163	31272	1542	11346
	%	35.37	45.77	2.26	16.61
2002	Ha	26992	28959	1218	11153
	%	39.51	42.39	1.80	16.32
2006	Ha	29535	19696	1073	18017
	%	43.23	28.83	1.57	26.37
2009	Ha	39910	11153	489	16785
	%	58.40	16.32	0.72	24.56

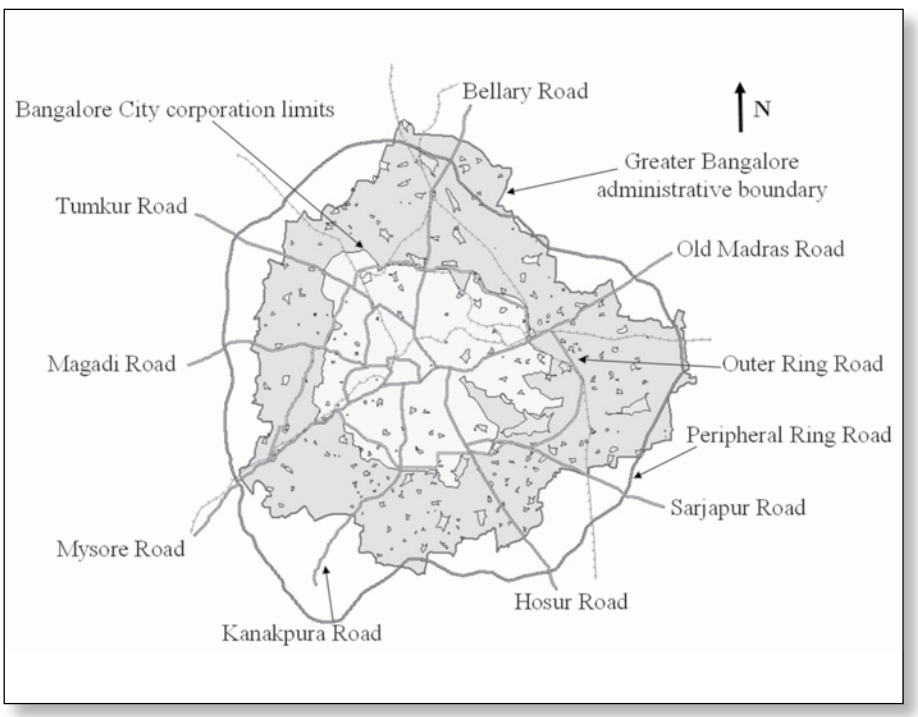

Figure 4: Greater Bangalore with 265 water bodies.

LST were computed from Landsat TM and ETM thermal bands. The minimum and maximum temperature from Landsat TM data of 1992 was 12 and 21 with a mean of 16.5±2.5 while for ETM+ data was 13.49 and 26.32 with a mean of 21.75±2.3. MODIS Land Surface Temperature/Emissivity (LST/E) data with 1 km spatial resolution with a data type of 16-bit unsigned integer were multiplied by a scale factor of 0.02 (http://lpdaac.usgs.gov/modis/dataproducts.asp#mod11). The corresponding temperatures for all data were converted to degree Celsius. Figure 5 shows the LST map and NDVI of Greater Bangalore in 1992, 2000 and 2007. The minimum (min) and maximum (max) temperatures were computed as 20.23, 28.29 and 23.79, 34.29 with a mean of 23.71±1.26, 28.86± 1.60 for 2000 and 2007 respectively. Data were calibrated with in-situ measurements. NDVI was computed to study its relationship with LST. The Landsat TM NDVI had a mean of 0.04±0.4543, ETM+ data had a mean of 0.0252±0.5369 and MODIS had a mean of -0.0917±0.5131.

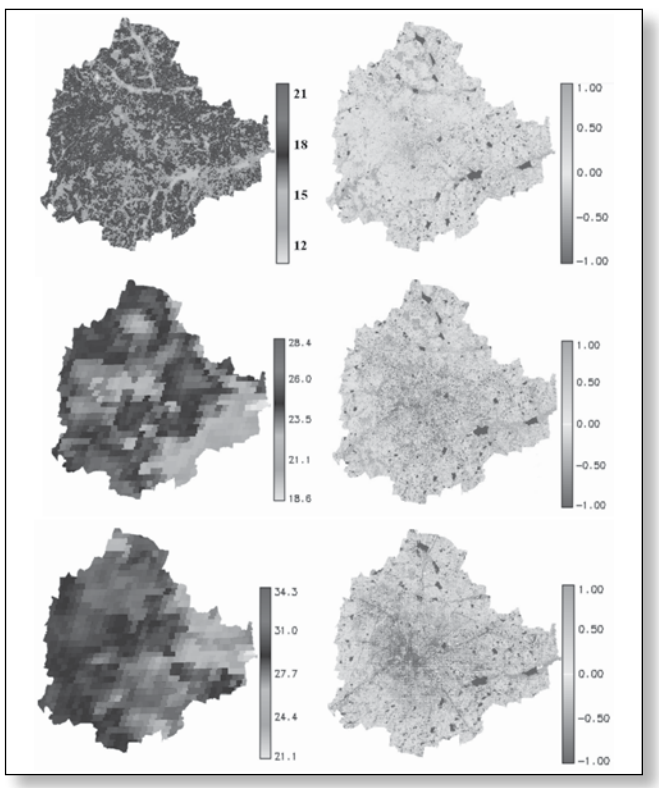

Figure 5: LST and NDVI from Landsat TM (1992), MODIS (2002 and 2007).
(Note: pixelisation of MODIS 2002 and 2007 is mainly due to coarse spatial resolution ~ 1 Km)

The correlation between NDVI and temperature of 1992 TM data was 0.88, 0.72 for MODIS 2000 and 0.65 for MODIS 2007 data respectively, suggesting that the extent of LC with vegetation plays a significant role in the regional LST. Respective NDVI and LST for different land uses is given in table 3 and further analysis was carried out to understand the role of respective land uses in the regional LST's.

***Table 3**: LST (°C) and NDVI for various land uses.*

Land use	1992 (TM)		2000 (MODIS)		2007 (MODIS)	
	LST	NDVI	LST	NDVI	LST	NDVI
	± SD	±SD	± SD	±SD	± SD	±SD
Builtup	19.03	-0.162	26.57	-0.614	31.24	-0.607
	±1.47	±0.096	±1.25	±0.359	±2.21	±0.261
Vegetation	15.51	0.467	22.21	0.626	25.79	0.348
	±1.05	±0.201	±1.49	±0.27	±0.44	±0.42
Water bodies	12.82	-0.954	21.27	-0.881	24.20	-0. 81
	±0.62	±0.055	±1.03	±0.045	±0.27	±0.27
Open ground	17.66	-0.106	24.73	-0.016	28.85	-0.097
	±2.46	±0.281	±1.56	±0.283	±1.54	±0.18

It is clear that urban areas that include commercial, industrial and residential land exhibited the highest temperature followed by open ground. The lowest temperature was observed in water bodies across all years and vegetation. Spatial variation of NDVI is not only subject to the influence of vegetation amount, but also to topography, slope, solar radiation availability, and other factors (Walsh *et al*., 1997). The relationship between LST and NDVI was investigated for each LC type through the Pearson's correlation coefficient at a pixel level and are listed in table 4. The significance of each correlation coefficient was determined using a one-tail Student's t-test. It is apparent that values tend to negatively correlate with NDVI for all LC types. NDVI values for built up ranges from -0.05 to -0.6. Temporal increase in temperature with the increase in the number of urban pixels during 1992 to 2009 (113%) is confirmed with the increase in 'r' values for the respective years. The NDVI for vegetation ranges from 0.15 to 0.6. Temporal analyses of the vegetation show a decline of 65%, with a consequent increase in the temperature.

A closer look at the values of NDVI by LULC category (table 3) indicates that the relationship between LST and NDVI may not be linear. Clearly, it is necessary to further examine the

***Table 4**: Correlation coefficients between LST and NDVI by LC type (p=0.05)*

Land use	1992	2000	2007
Built up	-0.7188	-0.7745	-0.7900
Vegetation	-0.8720	-0.6211	-0.6071
Open ground	-0.6817	-0.5837	-0.6004
Water bodies	-0.4152	-0.4182	-0.4999

existing LST and vegetation abundance relationship using fraction as an indicator. The abundance images using linear unmixing from ETM+ bands were further analysed to see their contribution to the UHI by separating the pixels that contains 0-20%, 20-40%, 40-60%, 60-80% and 80-100% of urban pixels. Table 5 gives the average LST for various land use classes.

***Table 5**: Mean LST for various land use classes for different abundances*

Class → Abundance ↓	Mean Temperature± SD of dense urban	Mean Temperature± SD of mixed urban	Mean Temperature± SD of vegetation
0-20%	21.99±2.37	21.57±2.36	17.91±2.19
20-40%	22.06±2.15	21.58±2.36	17.39±1.37
40-60%	22.27±2.00	21.67±2.41	17.22±0.89
60-80%	22.33 ±2.22	22.28±2.02	17.13±0.85
80-100%	22.47±1.96	22.37±2.17	17.12±0.91

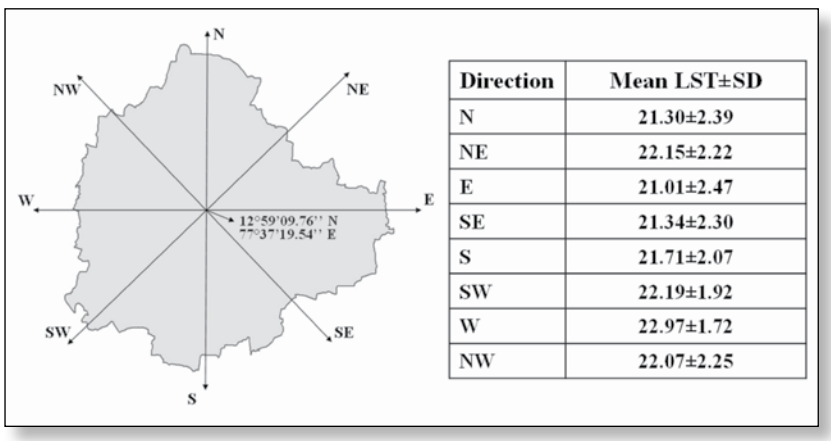

Direction	Mean LST±SD
N	21.30±2.39
NE	22.15±2.22
E	21.01±2.47
SE	21.34±2.30
S	21.71±2.07
SW	22.19±1.92
W	22.97±1.72
NW	22.07±2.25

Figure 6: Transect lines superimposed on Greater Bangalore boundary along with LST in various directions.

8 transacts were laid across the city in different directions (north [N], north-east [NE], east [E], south-east [SE], south [S], south-west [SW], west [W] and north-west [NW]) and LST was analysed as shown in figure 6, to understand the temperature dynamics.

The temperature profile was analysed by overlaying the LST map on the Baye's classified map to visualise the effect of vegetation, builtup, water bodies and open ground. The temperature profile plot fell below the mean when a vegetation patch or water body was encountered on the transact beginning from the center of the city and moving outwards along the transact. The corresponding graphs are shown in figure 7. The major natural green area and water bodies responsible for temperature decline are marked with circle. The spatial location of these green areas and water bodies are shown in figure 8.

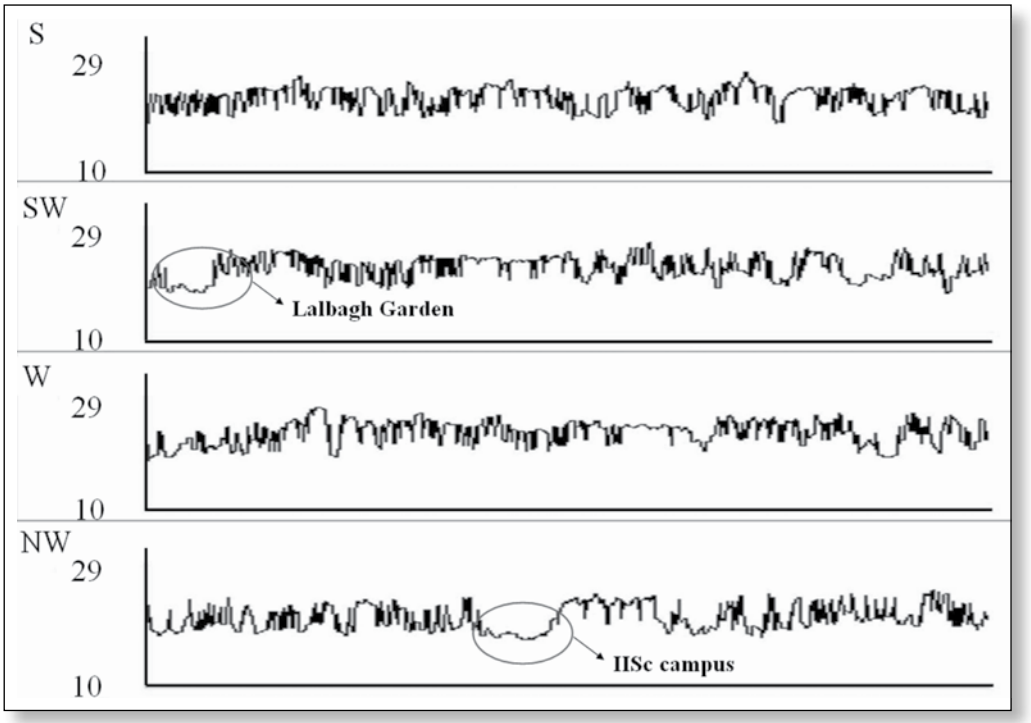

Figure 7: Temperature profile in various directions. X axis – Movement along the transacts from the city centre, Y axis - Temperature (°C).

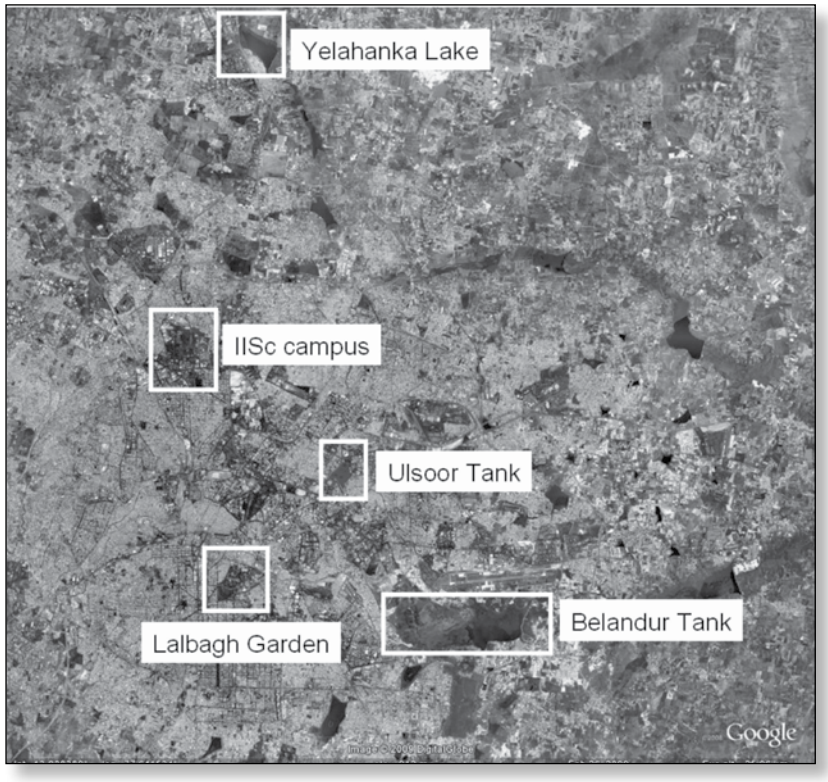

Figure 8: Google Earth image showing the low temperature areas (refer figure 7). [Source: http://earth.google.com/]

Conclusion

Urbanisation and the consequent loss of lakes has led to decrease in catchment yield, water storage capacity, wetland area, number of migratory birds, flora and fauna diversity and ground water table. As land is converted, it loses its ability to absorb rainfall. The relationship between LST and NDVI investigated through the Pearson's correlation coefficient at a pixel level and the significance tested through one-tail Student's t-test, confirms the relationship for all LC types. Also, increased urbanisation has resulted in higher population densities in certain wards, which incidentally have higher LST due to high level of anthropogenic activities. The growth poles are towards N, NE, S and SE of the city indicating the intense urbanization process due to growth agents like setting up of IT corridors, industrial units, etc. Newly builtup areas in these regions consisted of maximum number of small-scale industries, IT companies, multistoried building and private houses that came up in the last one decade.

The growth in northern direction can be attributed to the new International Airport, encouraging other commercial and residential hubs. The southern part of the city is experiencing new residential and commercial layouts and the north-western part of the city outgrowth corresponds to the Peenya industrial belt along with the Bangalore-Pune National Highway

Acknowledgement

We thank the Ministry of Environment and Forests, Government of India, Indian Institute of Science and the Ministry of Science and Technology, DST, Government of India for the sustained financial and infrastructure support to energy and wetlands research.

References

- Artis, D. A., and Carnahan, W. H. (1982). Survey of emissivity variability in thermography of urban areas. *Remote Sensing of Environment* 12: 13-329.
- Kulkarni, V. and Ramachandra T.V. (2006). *Environmental Management*, Commonwealth Of Learning, Canada and Indian Institute of Science, Bangalore.
- Landsat Project Science Office. (2002). Landsat 7 science data user's handbook. Goddard Space Flight Center, Available from: www.address: http://ltwww.gsfc.nasa.gov/IAS/handbook/ handbook_toc.html.
- Li, F., Jackson, T. J., Kustas, W, Schmugge, T., J., French, A. N., Cosh, M. L., and Bindlish, R. (2004). Deriving land surface temperature from Landsat 5 and 7 during SMEX02/SMACEX. *Remote Sensing of Environment* 92: 521-534.
- Nikolakopoulos, K. G, Vaiopoulos, D. A, Skianis, G. A. (2003). Use of multitemporal remote sensing thermal data for the creation of temperature profile of Alfios river basin. *Geoscience and Remote Sensing Symposium, 21-25 July 2003, IGARSS '03. Proceedings,IEEE International*, 4: 2389-2391.
- Ramachandra T V and Uttam Kumar (2009). Land surface temperature with land cover dynamics: multi-resolution,spatio-temporal data analysis of Greater Bangalore, International Journal of Geoinformatics, 5 (3):43-53
- Ramachandra T.V and Uttam Kumar (2008). Wetlands of Greater Bangalore, India: Automatic Delineation through Pattern Classifiers, *The Greendisk Environmental Journal*. Issue 26 (International Electronic Jour. URL: (http://egj.lib.uidaho.edu/index.php/egj/article/view/3171).
- Ramachandra T.V. and Shwetmala (2009). Emissions from India's Transport sector: Statewise Synthesis, *Atmospheric Environment*, 43 (2009) 5510–5517.
- Singh, S., M. (1998). Brightness Temperatures Algorithms of Landsat Thematic Mapper Data. *Remote Sensing of Environment* 24: 509-512.

- Snyder, W. C., Wan, Z., Zhang, Y., and Feng, Y. -Z. (1998). Classification based emissivity for land surface temperature measurement from space. *International Journal of Remote Sensing* 19: 2753-2774.
- Sobrino, J. A., and Raissouni, N. (2000). Toward remote sensing methods for land cover dynamic monitoring: Application to Morocco. *International Journal of Remote Sensing* 21: 353-366.
- Stathopoplou, M., Cartalis, C. and Petrakis, M. (2006). Integrating CORINE land cover data and landsat TM for surface emissivity definitions: an application for the urban area of Athens, Greece, *International Journal of Remote Sensing*.
- Stathopoulou, M., and Cartalis, C. (2007). Daytime urban heat island from Landsat ETM+ and Corine land cover data: An application to major cities in Greece. *Solar Energy* 81: 358-368.
- Streutker, D. R. (2002). A remote sensing study of the urban heat island of Houston, Texas. *International Journal of Remote Sensing* 23: 2595-2608.
- Sudhira H.S., Ramachandra T.V., Bala Subramanya M.H. (2007). City Profile: Bangalore., *Cities* l24(4): 379-390.
- Sudhira, H.S., Ramachandra, T.V., and Jagadish, K. S. (2003). Urban sprawl: metrics, dynamics and modelling using GIS, *International Journal of Applied Earth Observation and Geoinformation* 5(2004): 29-39.
- Walsh, S. J., Moody, A., Allen, T. R., and Brown, D. G. (1997). Scale dependence of NDVI and its relationship to mountainous terrain. In D. A. Quattrochi, & M. F. Goodchild (Eds.), Scale in Remote Sensing and GIS, pp. 27-55, Boca Raton, FL: Lewis Publishers.
- Weng, Q. (2001). A remote sensing-GIS evaluation of urban expansion and its impact on surface temperature in the Zhujiang Delta, China. *International Journal of Remote Sensing* 22: 1999-2014.
- Weng, Q. (2003). Fractal analysis of satellite-detected urban heat island effect. *Photogrammetric Engineering and Remote Sensing* 69: 555-566.
- Weng, Q., Lu, D., and Schubring, J. (2004). Estimation of land surface temperature – vegetation abundances relationship for urban heat island studies. *Remote Sensing of Environment* 89: 467-483.
- World Urbanization Prospects. (2005). Revision, Population Division, Department of Economic and Social Affaris, UN.